Roles of Achaete-Scute Homologue 1 in DKK1 and E-cadherin Repression and Neuroendocrine Differentiation in Lung Cancer

Hirotaka Osada,[1,2] Shuta Tomida,[3] Yasushi Yatabe,[4] Yoshio Tatematsu,[1] Toshiyuki Takeuchi,[3] Hideki Murakami,[1] Yutaka Kondo,[1] Yoshitaka Sekido,[1] and Takashi Takahashi[3]

[1]Division of Molecular Oncology, Aichi Cancer Center Research Institute; [2]Department of Cellular Oncology and [3]Division of Molecular Carcinogenesis, Center for Neurological Diseases and Cancer, Nagoya University Graduate School of Medicine; [4]Department of Pathology and Molecular Diagnostics, Aichi Cancer Center Hospital, Nagoya, Japan

Abstract

The proneural basic-helix-loop-helix protein achaete-scute homologue 1 (ASH1) is expressed in a very limited spectrum of normal and cancerous cells in a lineage-specific manner, including normal pulmonary neuroendocrine cells and lung cancer cells with neuroendocrine features. Our previous results indicated that ASH1 may play a crucial role in the growth and survival of lung cancers with neuroendocrine features, which prompted us to investigate the molecular function of ASH1 in relation to its involvement in carcinogenic processes. Herein, we report for the first time that ASH1 functions as a dual transcription factor by activating neuroendocrine differentiation markers and also repressing putative tumor suppressors. This protein was found to inactivate DKK1 and DKK3, negative regulators of Wnt/β-catenin signaling, E-cadherin, and integrin β1 through ASH1-mediated deacetylation and repressive trimethylation of lysine 27 (H3K27me3) of histone H3 in the promoter regions of DKK1 and E-cadherin. In addition, ASH1-transduced A549 adenocarcinoma cells exhibited markedly altered morphology characteristics compared with lung cancer cells with neuroendocrine features both *in vitro* and *in vivo* and also grew faster *in vivo*. Our results provide important clues for a better understanding of the molecular and cellular biological roles of ASH1 in the process of carcinogenesis of lung cancers with neuroendocrine features and warrant future investigations to shed light on the lineage-specific dependency of this transcription factor with dual functions. [Cancer Res 2008;68(6):1647–55]

Introduction

Lung cancer has long been the leading cause of cancer-related death in many economically developed countries, and a better understanding of the molecular pathogenesis of this fatal disease is greatly anticipated for preventive and/or therapeutic breakthroughs to drastically reduce the rate of mortality (1). Lung cancer is classified into two major classes, small cell lung cancer (SCLC) and non-SCLC (NSCLC), based on the clinicopathologic characteristics, whereas the latter is further divided into three major types of tumors with distinct morphologic features, adenocarcinomas, squamous cell carcinomas, and large cell carcinomas. It has also been well recognized that there are distinct types of lung tumors that exhibit neuroendocrine features, which comprise SCLCs and subsets of large cell carcinomas, such as large cell neuroendocrine carcinoma (LCNEC) and carcinoids. Although LCNEC is considered to be a disease entity distinct from SCLC, these two types of lung cancers share a great number of features, such as expression profiles and clinical characteristics (2–4), which suggest the possible roles of one or more genes related to neuroendocrine differentiation in the carcinogenic processes.

Achaete-scute homologue 1 (ASH1) is a basic-helix-loop-helix protein that is expressed in normal pulmonary neuroendocrine cells (PNEC) and lung cancers with neuroendocrine features (5, 6). PNECs are proposed to play important roles in the development and growth regulation of lung epithelial cells by functioning as a stem-cell niche and chemoreceptors. It was previously shown that gene targeting of *ASH1* resulted in loss of PNECs in the lung (7), whereas an *ASH1* transgene promoted the development of lung tumors with neuroendocrine features in cooperation with SV40 large T antigen (8). We also reported that suppression of ASH1 expression by RNA interference induced cell cycle arrest and apoptosis *in vitro* and inhibited growth of lung cancer cells *in vivo* in an ASH1 expression-dependent manner (9), leading us to propose that ASH1 may be involved in "lineage-specific" survival and growth of lung cancers with neuroendocrine differentiation (10). However, the molecular mechanisms underlying the distinctive features of lung cancers expressing ASH1 remain largely unresolved.

In the present study, we aimed to elucidate the molecular functions of ASH1 in relation to its involvement in the carcinogenic processes of lung cancers with neuroendocrine differentiation. Herein, we report for the first time that ASH1 functions as a transcription factor with dual functions, leading to activation of neuroendocrine differentiation markers, as well as repression of putative tumor suppressors, including the Wnt signaling inhibitors DKK1 and DKK3, E-cadherin, and integrin β1. We also found that transcriptional repression of *DKK1* and *E-cadherin* was associated with histone deacetylation and accelerated histone H3 lysine 27 trimethylation (H3K27me3). Together with our findings showing the biological effects of ASH1 expression *in vitro* and *in vivo*, these results provide important clues for a better understanding of how ASH1 may contribute to the development and acquisition of malignant properties of high-grade neuroendocrine lung tumors, such as SCLC and LCNEC.

Materials and Methods

Expression constructs. For the construction of expression plasmids, *ASH1, DKK1, LEF1, HDAC1*, and *HDAC3* cDNAs were generated with reverse transcription–PCR (RT-PCR) and inserted into pCMV-puromycin or pcDNA3 (Invitrogen). For construction of lentivirus vectors, *ASH1* and *DKK1* cDNAs were inserted into CSII-CMV-MCS-IRES2-Blasticidin and

Note: Supplementary data for this article are available at Cancer Research Online (http://cancerres.aacrjournals.org/).

Requests for reprints: Hirotaka Osada, Division of Molecular Oncology, Aichi Cancer Center Research Institute, 1-1 Kanokoden, Chikusa-ku, Nagoya 464-8681, Japan. Phone: 81-52-764-2993; Fax: 11-81-52-764-2993; E-mail: hosada@aichi-cc.jp.

doi:10.1158/0008-5472.CAN-07-5039

CSII-EF-MCS-IRES2-Venus (improved YFP) vectors, respectively, which were kindly provided by Dr. H. Miyoshi (RIKEN BioResource Center). Venus was provided by Dr. A. Miyawaki (RIKEN Brain Science Institute). The myc-tag was attached at the NH_2 terminus of *ASH1* cDNA. Lentiviruses were produced according to the protocol of Dr. Miyoshi. The constructed vectors were cotransfected with pCAG-HIVg and pCMV-VSV-G-RSV-Rev plasmids into 293T cells. Two days after transfection, the supernatant was harvested and concentrated using ultracentrifugation. The virus particle pellets were resuspended in RPMI medium and stored at −80°C. The virus titer was determined by counting Venus-positive cells or Blasticidin-resistant colonies. A549 cells were infected with *ASH1* or empty lentiviruses. After infection, the cell lysates were consecutively harvested, and total RNA was extracted using an RNeasy kit (Qiagen), according to the manufacturer's instructions.

Expression profiling with microarrays. Using the RNA samples of both A549-ASH1 and A549-VC cells at 4 d after infection, cRNA was generated and labeled with Cy3 or Cy5 (GE Healthcare) using a low RNA fluorescent linear amplification kit (Agilent Technologies), according to the manufacturer's instructions. Labeled cRNAs were hybridized to an Agilent 44K whole human genome microarray, followed by confocal laser scanning (Agilent Technologies). Duplicate experiments of expression profiling were performed.

Luciferase assay. For analysis of β-catenin/TCF activity, TOP-flash and FOP-flash reporters (pGL3-OT with three wild-type TCF/LEF sites and pGL3-OF with mutated TCF/LEF sites, respectively, kindly provided by Dr. B. Vogelstein) were used. For generation of *DKK1* and *E-cadherin* reporter constructs, genomic fragments corresponding to *DKK1* (1,007 bp) and *E-cadherin* (364 bp) promoters were amplified with PCR and inserted into a pGL3 basic reporter (Promega). E-box motifs were disrupted using PCR amplification with Pfu TURO (Stratagene) and primers containing mismatches at E-box motifs. Luciferase reporter activity was measured as previously described in detail (11). In brief, A549 cells were grown at 3×10^5 in a 3-cm dish and transfected in triplicate with 0.6 μg of the expression vector, along with 0.02 μg of a firefly luciferase reporter (TOP-flash, DKK1, or E-cadherin reporter) and 0.01 μg of an internal control reporter, pRL-TK (Promega) using Lipofectamine 2000 (Invitrogen). To assess β-catenin/TCF activities, A549-ASH1 or A549-VC cells were transfected with a TOP-flash or FOP-flash reporter. The day after transfection, firefly luciferase and *Renilla* luciferase activities were measured using a dual-luciferase reporter assay system (Promega). Firefly luciferase activity was normalized with that of *Renilla* luciferase.

Chromatin immunoprecipitation assay. A chromatin immunoprecipitation (ChIP) assay was performed basically as described previously (11). Before harvesting, cells were treated with 1% formaldehyde for 10 min at 37°C, then harvested, and resuspended in SDS lysis buffer [1% SDS, 10 mmol/L EDTA, and 50 mmol/L Tris-HCl (pH 8.1)] for 10 min on ice. After a brief sonication, antibodies (Upstate Biotechnology) were added to the lysate. After an overnight incubation, immune complexes were collected using protein G-Sepharose 4 fast flow. The immunoprecipitated protein-DNA complexes were eluted with SDS/sodium bicarbonate and extracted using standard proteinase K/phenol extraction procedures. The obtained DNA was PCR-amplified using semiquantitative PCR with Platinum Taq DNA polymerase (Invitrogen) and primers for *DKK1, E-cadherin, chromogranin B (CHGB), secretogranin 2 (SCG2)*, and *β-actin* promoters, applied using electrophoresis and measured with an ImageMaster-CL densitometer (GE Healthcare). The amount of DNA was also determined using real-time PCR with Power SYBR Green PCR Master Mix (Applied Biosystems) and a 7500 Real-Time PCR System (Applied Biosystems). The amounts of each promoter were normalized by that of the *β-actin* promoter and then compared between A549-ASH1 and A549-VC cells. In a ChIP assay of the *DKK1* promoter of SCLC cell lines, the amount of *DKK1* promoter was similarly normalized with that of the *β-actin* promoter, and its ratio to whole cell extract is presented. Both analyses showed consistent results. The antibodies used were anti–acetyl-histone H3 (K^9/K^{14}), anti–acetyl-H3 (Lys^9), anti–dimethyl-H3 (Lys^4), anti–trimethyl-H3 (Lys^4), anti–dimethyl-H3 (Lys^9), anti–trimethyl-H3 (Lys^9), anti–monomethyl-H3 (Lys^{27}), and anti–trimethyl-H3 (Lys^{27}) antibodies (Upstate). For immunoprecipitation of ASH1, the anti–myc-tag 9E10 antibody was used.

Results

Expression profiling of A549-ASH1 cell. To elucidate the molecular function of ASH1 in the carcinogenic processes of lung cancers with neuroendocrine differentiation, the *ASH1* gene was introduced into a typical adenocarcinoma cell line, A549, using an IRES-blasticidin lentiviral vector. Comparison of expression profiles between A549 cells transduced with an ASH1-expressing virus (A549-ASH1) and control virus-infected A549 cells (A549-VC) resulted in the identification of 219 and 67 genes with up-regulation and down-regulation, respectively (>4-fold; Supplementary Tables S1 and S2). Up-regulated genes included those directly related to neuroendocrine differentiation, such as *CHGB* and *SCG2*, whereas down-regulated genes comprised many that were related to cancer, including such putative tumor suppressors as *DKK1, DUSP1, RASSF2, E-cadherin, IGFBP6, SOCS3, DKK3*, and *SEMA3C*. Significant changes in the expression levels of *CHGB, SCG2, DKK1, DKK3, E-cadherin*, and *integrin β1* at various time points after transduction of the ASH1-expressing virus were further substantiated by quantitative RT-PCR analysis (Figs. 1*A*, 3*A, left,* and 4*A*). The whole results of duplicate microarray analyses of A549-ASH1 and A549-VC cells are also presented in Supplementary Table S4.

ASH1-mediated repression of DKK1. Identification of significant down-regulation of the DKK1 and DKK3 Wnt signaling inhibitors prompted us to investigate the molecular and biological consequences of ASH1-mediated transcriptional repression. We observed that introduction of DKK1 significantly inhibited the growth of an ASH1-expressing and DKK1-repressed SCLC cell line, ACC-LC-172, whereas A549 cells, which express endogenous DKK1 but not ASH1, did not show any inhibited growth (Fig. 1*B, top*). Similarly, ACC-LC-80 with repressed DKK1 showed a significant reduction of Venus fluorescence intensity, which reflected the fraction of virus-infected cells indicated by the DKK1-IRES-Venus lentivirus, in contrast to virtually no effect in ACC-LC-76 expressing endogenous DKK1 (Fig. 1*B, bottom*). These results clearly showed the growth inhibitory effects of DKK1 in DKK1-negative and ASH1-positive lung cancer cells, suggesting a functional consequence of DKK1 down-regulation in association with ASH1 expression.

It is possible that the down-regulation of DKK1 might be indirect, thus reflecting an inactivated state of Wnt/β-catenin signaling imposed by ASH1 expression, because it is known that DKK1 can be activated through a negative feedback mechanism in the Wnt/β-catenin signaling pathway. As shown in Fig. 1*C* (*top left*), ASH1 indirectly activated a TOP-flash reporter, which contains three TCF/LEF sites, but not a FOP-flash reporter in A549 cells. We also found that ASH1 expression did not affect activation by LEF1, a Wnt/β-catenin signaling mediator (Fig. 1*C, top right*). These findings indicate that ASH1 is able to activate the Wnt/β-catenin signaling pathway and DKK1 repression is unlikely to be a consequence of Wnt/β-catenin inactivation.

We also studied the activity of the *DKK1* promoter, which contains Wnt/β-catenin signal-responsive TCF/LEF sites and a possible ASH1-binding element, E-box. *DKK1* promoter activity was clearly down-regulated by ASH1 in A549 cells (Fig. 1*C, bottom left*), whereas LEF1 activated the *DKK1* reporter, which is a negative feedback mechanism. Notably, LEF1-mediated activation of the *DKK1* reporter, which contains both TCF/LEF-binding and ASH1-binding sites, was significantly inhibited by ASH1 (Fig. 1*C, bottom right*), in contrast to the results with the TOP-flash reporter shown in Fig. 1*C* (*top right*). Together with the lack of any physical interaction between ASH1 and either β-catenin or LEF1 (data not

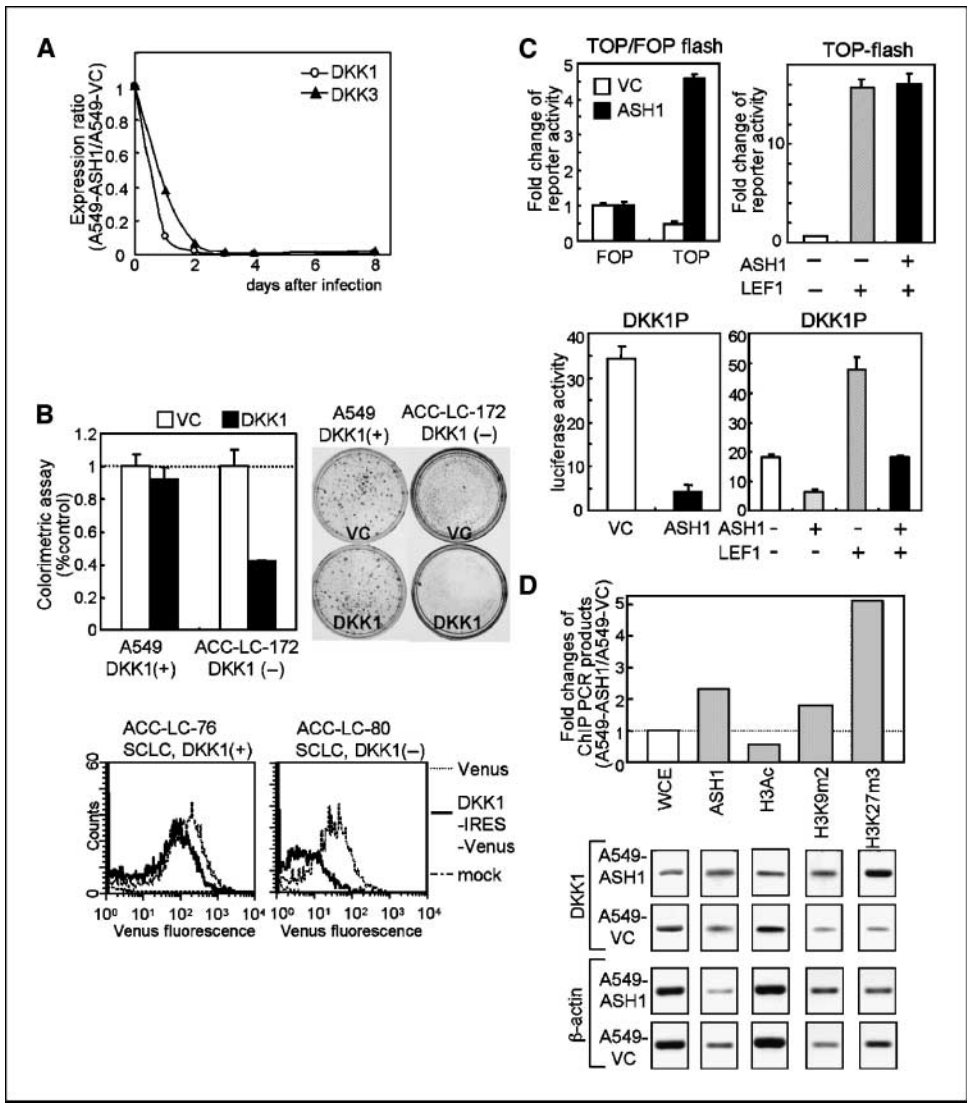

Figure 1. ASH1-mediated repression of DKK1-inhibited cell growth of DKK1-negative SCLC cells. *A,* quantitative RT-PCR analysis of DKK1 and DKK3 with A549-ASH1 cells, showing prompt repression after infection with the ASH1-expressing virus. *B, top,* cell growth was significantly reduced by transfection of ASH1 into ACC-LC-172 SCLC cells lacking DKK1 expression, but not A549 adenocarcinoma cells expressing DKK1, as measured by a colorimetric assay (*left*) and colony formation assay (*right*). *B, bottom,* Venus fluorescence intensity reflecting cell growth was significantly reduced in ACC-LC-80 SCLC cells with DKK1 silencing after infection with the DKK1-IRES-Venus lentivirus. Virtually, no effect was observed in ACC-LC-76 SCLC cells expressing DKK1. *C, top,* TOP-flash/FOP-flash assays, showing strong enhancement with the TOP-flash reporter containing TCF/LEF-responsive elements in A549-ASH1, but not A549-VC cells. *C, top right,* TOP-flash assay of A549 cells transfected with ASH1 and/or LEF1, showing no effect of ASH1 on LEF1-mediated activation of the TOP-flash reporter. *C, bottom,* reporter assay of the DKK1 promoter containing both TCF/LEF sites and a possible ASH1-binding E-box. Marked inhibition was seen with the introduction of ASH1. Note that LEF1-induced activation of the DKK1 reporter was also suppressed by ASH1. *D,* ChIP assays of the DKK1 promoter in A549-ASH1 and A549-VC cells, showing significant deacetylation and induction of H3K27me3 in A549-ASH1 cells. The ratios of the DKK1 PCR products between A549-ASH1 and A549-VC cells are shown after normalization with β-actin PCR products (*top*) and each PCR product is also shown (*bottom*). The ratio of PCR products with whole cell extracts (*WCE*) was set at 1.

shown), these findings suggest a direct inhibitory effect of ASH1 on DKK1 expression.

We did not observe changes in the DNA methylation status of the *DKK1* promoter region in A549-ASH1 cells (data not shown), whereas significant changes in the chromatin structure of the *DKK1* promoter were found (Fig. 1*D*). The results of a ChIP assay clearly showed direct binding of ASH1 to the *DKK1* promoter, as well as transcription-repressing histone deacetylation and trimethylation of Lys^{27} (H3K27me3) of histone H3 in A549-ASH1 cells. In addition, ASH1 was shown to form a complex with HDAC1 and HDAC3 (Supplementary Fig. S1*A*). Taken together, these findings strongly suggest that ASH1 has the ability to directly bind to the *DKK1* promoter, which in turn recruits histone-modifying molecules, consequently inducing transcriptional repression of the *DKK1* promoter. Because H3K27me3 is mainly catalyzed by EZH2 in the polycomb-repressing complex (12), the interaction between ASH1 and EZH2 was also studied. However, no clear evidence of such interaction was detected (data not shown).

DKK1 silencing in SCLC cell lines and tumor tissues. Next, we investigated whether the expression level of DKK1 had a relationship with that of ASH1 in lung cancer cell lines *in vitro*, as well as in lung cancer tumor specimens. DKK1 expression in SCLC cells with a generally high level of ASH1 expression was significantly lower than that in NSCLC (adenocarcinomas and squamous cell carcinoma) cell lines (Fig. 2*A*), whereas DKK1 downregulation was also observed in SCLC tumor specimens, but not in tumor tissues from adenocarcinomas and squamous cell carcinomas (Fig. 2*B*), demonstrating clear inverse correlations both *in vitro* and *in vivo*. DNA methylation of the *DKK1* promoter region was also studied using a panel of lung cancer cell lines with methylation-specific PCR (MSP) analysis, which resulted in identification of DNA methylation in the *DKK1* promoter in a limited fraction of cell lines, including cells from a single SCLC without DKK1 expression (Supplementary Fig. S1*B* and *C*). Analysis of the DNA methylation status at each CpG site in the representative cell lines yielded results consistent with those of MSP analysis (Fig. 2*C*; data not shown for A427). A ChIP assay was also performed, which showed the presence of histone deacetylation and induction of H3K27me3 in SCLC cell lines exhibiting DKK1 silencing without DNA methylation, whereas an SCLC cell line with DNA methylation, ACC-LC-80, exhibited induction of H3K9me2, but not H3K27me3 (Fig. 2*D*). These results suggest that

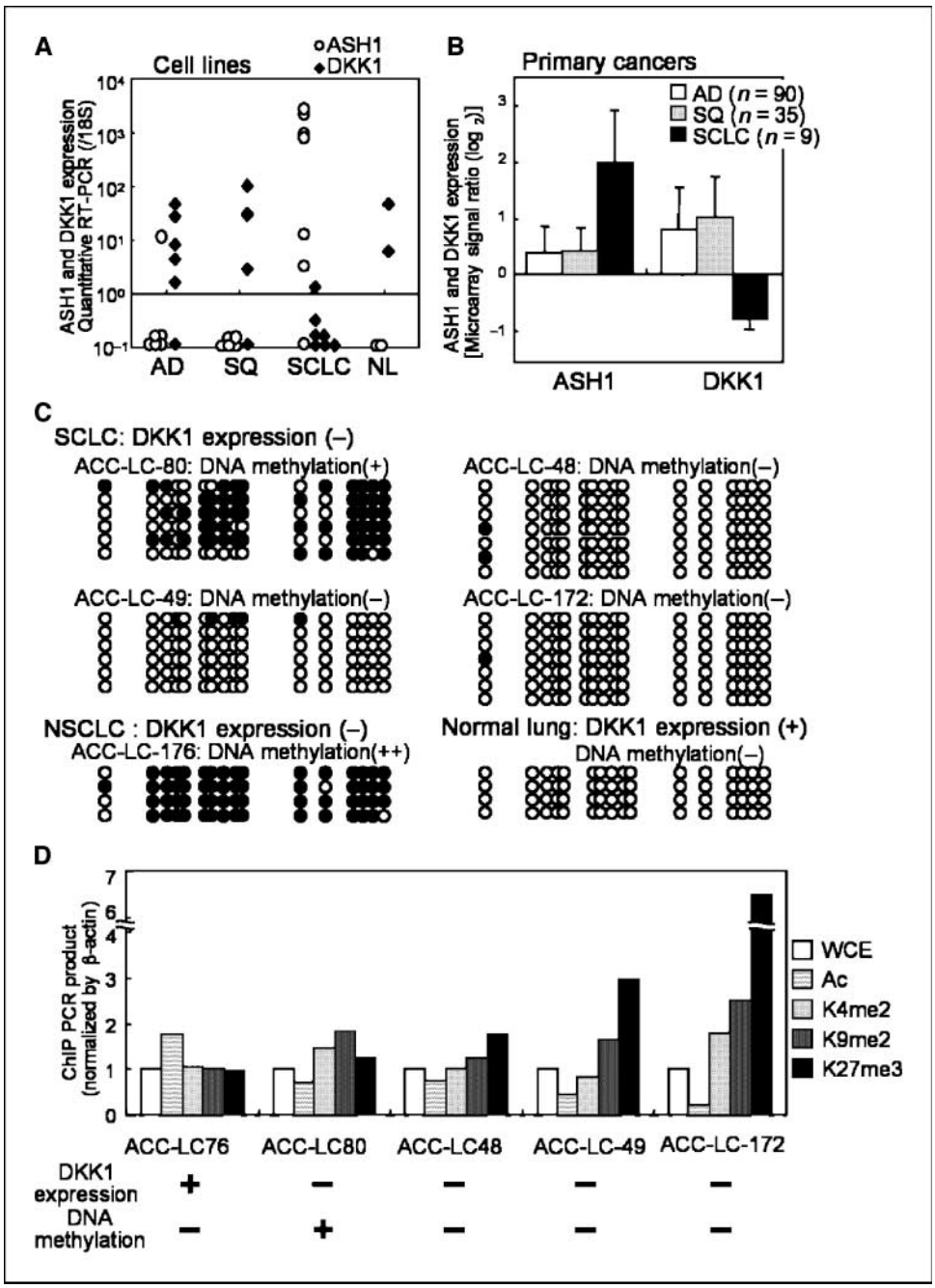

Figure 2. DKK1 silencing in SCLC cells and tumor tissues. *A,* inverse association between DKK1 and ASH1 expression in lung cancer cells, as determined by quantitative RT-PCR assays. *AD,* adenocarcinoma; *SQ,* squamous cell carcinoma. *B,* inverse association between DKK1 and ASH1 expression in primary lung cancers based on published microarray analysis data (29). *C,* bisulfite sequencing analysis of the DKK1 promoter in lung cancer cells and normal lung tissue, showing DNA methylation in a single SCLC cell line with DKK1 silencing. *Open circle,* nonmethylated CpG; *closed circle,* methylated CpG. *D,* ChIP assay of the DKK1 promoter in SCLC cells, showing histone H3 deacetylation in all SCLC cell lines with DKK1 silencing. H3K27me3 was seen in DKK-1–negative SCLC cell lines without DNA methylation.

DKK1 silencing in SCLCs is mainly attributable to repressive histone modifications imposed by ASH1 expression rather than DNA methylation.

Repression of E-cadherin by ASH1. We also studied the expression of E-cadherin and integrin β1, which are crucial regulators of cell-cell interactions. Quantitative RT-PCR analysis confirmed the results of the microarray analysis, showing down-regulation of E-cadherin and integrin β1 in response to introduction of ASH1 into A549 cells (Fig. 3*A, left*), whereas Western blot analysis also showed significant down-regulations of E-cadherin and integrin β1 proteins in ASH1-transduced A549 cells (Fig. 3*A, right*). The underlying mechanism for the transcriptional down-regulation of the *E-cadherin* gene was investigated using a luciferase reporter construct containing a PCR-amplified 369-bp-long genomic fragment of the *E-cadherin* promoter. Whereas ASH1 expression apparently reduced wild-type *E-cadherin* promoter activity, disruptions of E-boxes in the promoter region impaired the repressive effect of ASH1 (Fig. 3*B*).

Next, we turned our attention to the state of modification of the *E-cadherin* promoter in relation to transcriptional repression and found a lack of DNA methylation in ASH1-transduced A549 cells (data not shown). Then, the chromatin structure of the *E-cadherin* promoter was studied using a ChIP assay. ASH1 directly bound to the *E-cadherin* promoter and induced histone H3 deacetylation and H3K27me3 (Fig. 3*C*), as was similarly observed with the *DKK1* promoter. Interaction of ASH1 with E-box1 was shown by results of a gel shift assay using an E-box1 probe, which was completely competed out by a cold E-box oligonucleotide (Fig. 3*D*). Addition of

the antibody against myc-tag attached to the exogenous ASH1 protein clearly caused a super-shift of the band, implying binding of the ASH1 protein to the E-box1 element of the *E-cadherin* promoter. In contrast to the findings with the *DKK1* and *E-cadherin* genes, we observed the opposite effects of ASH1 with the neuroendocrine marker genes *CHGB* and *SCG2*. ChIP assay findings revealed that transduction of ASH1 in A549 cells led to induction of H3 acetylation and a reduction of H3K27me3 (Fig. 4*B*), resulting in a strong induction of CHGB and SCG2 expression (Fig. 4*A*).

ASH1-induced phenotypic changes *in vitro* and *in vivo*. Next, we investigated the phenotypic consequences of ASH1 expression in human lung cancer cells. In monolayer cultures (Fig. 5*A, top*), A549-VC cells tightly attached to the dishes like typical epithelial cells, whereas A549-ASH1 cells exhibited a round-shaped morphology with reduced cell adhesion. In semisolid cultures (Fig. 5*A, middle*), A549-VC cells formed compact cell aggregates, whereas A549-ASH1 cells had loose cell-cell contacts. Interestingly, three-dimensional cultures in collagen gels showed even greater morphologic differences between A549-VC and A549-ASH1, as A549-VC cells showed filopodia formation in contrast to the round-shaped cell morphology without any protrusions in A549-ASH1 cells (Fig. 5*A, bottom*). These ASH1-induced morphologic phenotypes closely resembled those of typically used SCLC cell lines, such as ACC-LC-48 (Fig. 5*A*). Immunofluorescent microscopic analysis

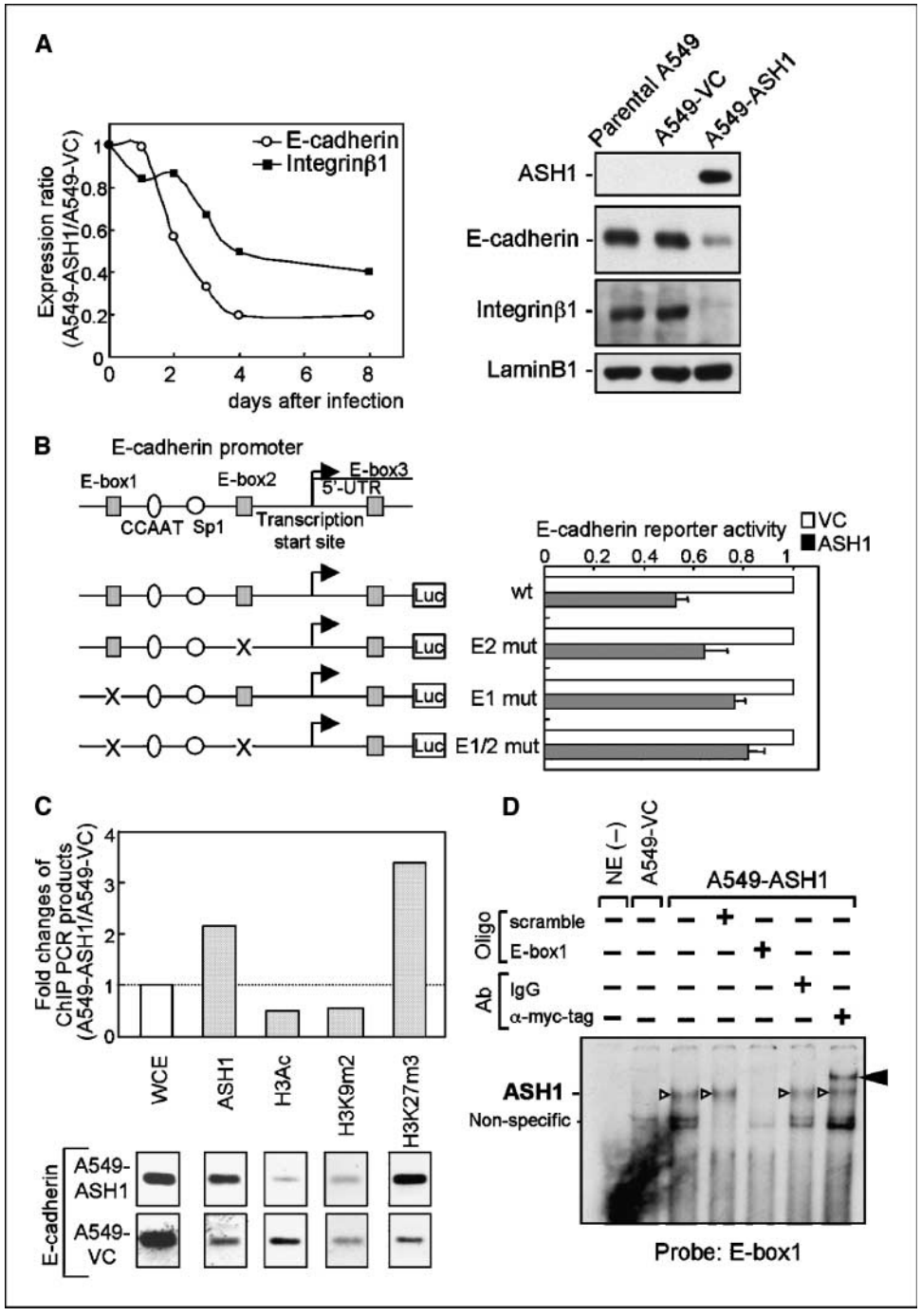

Figure 3. Transcriptional repression of E-cadherin by ASH1. *A, left,* quantitative RT-PCR analyses of E-cadherin and integrin β1 in A549-ASH1 cells, showing repression after transduction of the ASH1-expressing virus. *A, right,* Western blot analyses of E-cadherin and integrin β1, showing marked reduction in expression levels of E-cadherin and integrin β1 in A549-ASH1 cells. Lamin B1 served as the loading control. *B,* reporter assay of the E-cadherin promoter after cotransfection with the ASH1 expression vector (*gray column*) or control vector (*white column*), showing reduction of repression by introduction of mutations to the E-boxes in the promoter. A schematic diagram of the E-cadherin promoter reporters (*left*) with disrupted E-boxes indicated by an X. *Shaded boxes,* E-boxes; *ovals,* CCAAT-box; *circles,* SP1-consensus motif. *C,* ChIP assay of the E-cadherin promoter performed in a similar manner for analysis of the DKK1 promoter in Fig. 1, showing induction of deacetylation and H3K27me3 in A549-ASH1 cells. *D,* GEMSA assay, showing a shifted band (*open arrowheads*) specific to the A549-ASH1 nuclear extract. Note that the shifted band was clearly inhibited by the cold competitor of the E-box1 oligonucleotides, but not by scrambled oligo, and a supershift (*closed arrowhead*) was seen using the anti–myc-tag antibody for detecting myc-tagged ASH1.

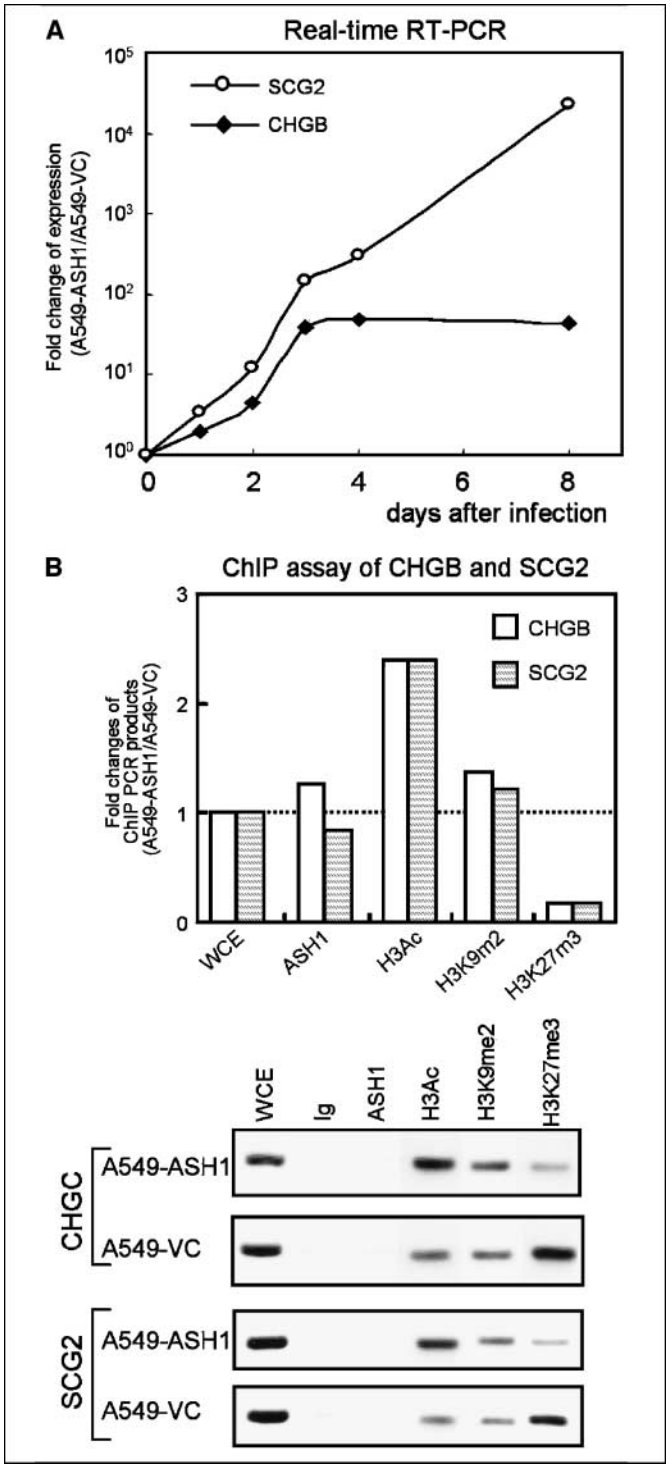

Figure 4. ASH1-mediated transcriptional activation of neuroendocrine markers. *A,* quantitative RT-PCR analyses of CHGB and SCG2 in A549-ASH1 cells, showing increased expression after ASH1 expression induced by viral infection. *B,* ChIP assay of the CHGB and SCG2 promoters. The results show the induction of acetylation and reduction of H3K27me3 in A549-ASH1 cells, which were in marked contrast to the DKK1 and E-cadherin promoters.

also showed abundant expression of E-cadherin on the cell surface of A549-VC, whereas that was scarcely observed on A549-ASH1 cells, suggesting that the phenotypical alterations may be attributable to markedly reduced expression of cell adhesion molecules (Fig. 5*B*). The effect of ASH1 on the subcellular localization of β-catenin was also studied using A549 cells transiently transfected with the ASH1 expression vector. Accumulation of β-catenin into the nuclei was observed in A549 cells expressing ASH1 (Fig. 5*C, arrowheads*), whereas nontransfected cells showed membrane-bound β-catenin proteins without nuclear accumulation, suggesting the activation of β-catenin signaling by ASH1.

We also examined the phenotypic consequences of ASH1 expression *in vivo* using A549-ASH1 and A549-VC xenografts. The former developed high-grade carcinomas with morphologic characteristics that showed neuroendocrine features, which are frequently seen in SCLCs, LCNECs, and carcinoid tumors. In contrast, tumors developed from the A549-VC xenografts formed cyst-like or tube-like structures, which were lined by columnar epithelia (Fig. 6*A*). Immunohistochemical analyses supported the morphologic characteristics, as a negative expression of E-cadherin and positive expression of neuroendocrine marker, known as synaptophysin, was observed in A549-ASH1 xenografts, whereas a contrasting pattern was observed in A549-VC xenografts (Fig. 6*B* and *C*). We also found accelerated tumor growth in A549-ASH1 xenografts compared with the A549-VC xenografts (Fig. 6*D*).

We also studied the universality and constancy of the effects of ASH1. In another adenocarcinoma cell line, SK-LC5, ASH1 overexpression induced alterations of gene expressions, i.e., down-regulation of DKK1 and up-regulation of SCG2 (Supplementary Fig. S2*A*), and the cells also underwent a phenotypic change into a round-shaped morphology (Supplementary Fig. S2*B*), similar to A549 cells, suggesting the universality of these ASH1 functions. In addition, dual-directional regulation of ASH1 on gene expression was consistently observed in stable A549-ASH1 cells when compared with the stable cell line A549-VC (Supplementary Fig. S2*C* and *D*), which was similar to the observation of early response just after virus infection.

Discussion

Our previous findings suggested an important role for ASH1 expression in lung cancers with neuroendocrine differentiation, including SCLCs and LCNECs (9), and led us to initiate the present study to elucidate the molecular function of ASH1 in relation to its involvement in carcinogenic processes. Our results showed a dual role of ASH1 as a transcriptional factor, leading to induction of a number of genes, such as neuroendocrine differentiation markers, as well as repression of multiple putative tumor suppressor genes, including the Wnt/β-catenin signaling inhibitors DKK1 and DKK3, as well as E-cadherin and integrin β1, which are cell adhesion molecules. In this regard, it should be noted that ASH1 is the first transcriptional repressor identified for members of the *DKK* gene family. We also showed that ASH1-mediated DKK1 and E-cadherin silencing were associated with the induction of histone H3 deacetylation and increased H3K27me3. Conversely, ASH1-mediated induction of neuroendocrine differentiation markers was associated with histone H3 acetylation and a reduction in H3K27me3.

Polycomb repressive complex 2 (PRC2), which induces H3K27me3, is thought to play important roles in stem cell biology. Gene silencing in stem cell–related genes is frequent in cancer cells and has been suggested to be a possible reflection of cell fate, which is preprogrammed through H3K27me3 by PRC2 (13–15). In this context, *DKK1* is a polycomb target gene and

repressed by H3K27me3 in ES cells (16, 17). ASH1 might play a role in carcinogenesis by expanding the population of cancer progenitor cells carrying preexisting H3K27me3, which may be in accordance with a hypothesis that PNEC is derived from multipotent epithelial progenitors that can differentiate into both Clara cells/pneumocytes and cells with a PNEC lineage (6). Alternatively, it is also possible that ASH1 may induce *de novo* H3K27me3, possibly through physical and/or functional interactions with PRC2.

Wnt signaling is thought to regulate the proliferation and renewal of stem cells, whereas dysregulated activation of Wnt/β-catenin signaling has been implicated in carcinogenesis (18). DKK1 inhibits Wnt/β-catenin signaling through disruption of the complex formation of Wnt and its receptors, LRP5/6 and Frizzled (19), whereas *DKK1* is transcriptionally induced by Wnt/β-catenin signaling itself as a negative feedback mechanism (20, 21). Evidence for the potential involvement of DKK1 inactivation in human cancers is accumulating. The *DKK1* gene was reported to be a frequent target for epigenetic silencing by DNA hypermethylation in colorectal cancers (21), whereas overexpression of DKK1 was shown to reduce *in vitro* and *in vivo* colorectal cancer cell growth (22). In contrast, the underlying mechanism of DKK1 silencing in lung cancers seems to be attributable mainly to repressive histone H3 modifications rather than DNA methylation, showing the existence of a lineage-specific preference imposed by the highly lineage-specific transcription factor ASH1. In addition to DKK1, we observed that ASH1 mediated the down-regulation of DKK3, which has also been reported to be inactivated in other cancers (19). Together with the increased growth of ASH1-transduced A549 cells, the present findings support the notion

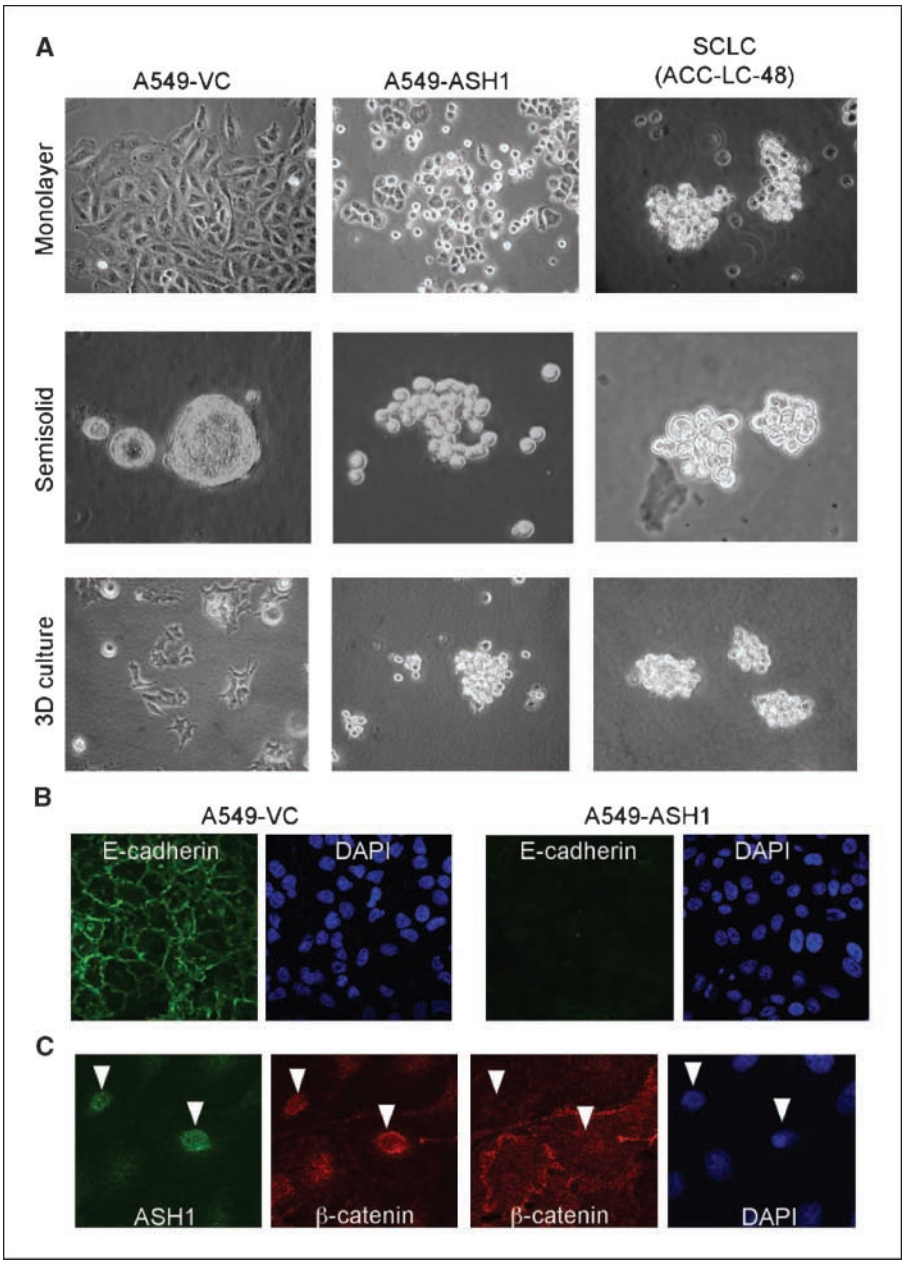

Figure 5. Phenotypic changes *in vitro* and *in vivo* in response to the introduction of ASH1 in A549 adenocarcinoma cells. *A, top,* induction of round-shaped morphology with a reduction of attachment to culture dishes in monolayer culture of A549-ASH1 cells. *A, middle,* induction of loose aggregate in semisolid culture of A549-ASH1 in contrast to compact cell aggregates of A549-VC. *A, bottom,* induction of round-shaped morphology without protrusion in three-dimensional culture of A549-ASH1 on collagen gels in contrast to filopodia formation by A549-VC. Note that a typical SCLC cell line, ACC-LC-48, shows complete anchorage-independence and loose cell-cell interactions similar to A549-ASH1. *B,* immunofluorescent staining of E-cadherin, showing loss of E-cadherin in A549-ASH1 in contrast to the abundant expression in A549-VC. *C,* immunofluorescent staining of β-catenin, showing induction of nuclear accumulation of β-catenin in ASH1-transfected A549 cells (*arrowheads*), suggesting the activation of β-catenin signaling. In contrast, plasma membrane-bound β-catenin is seen in cells lacking ASH1 expression.

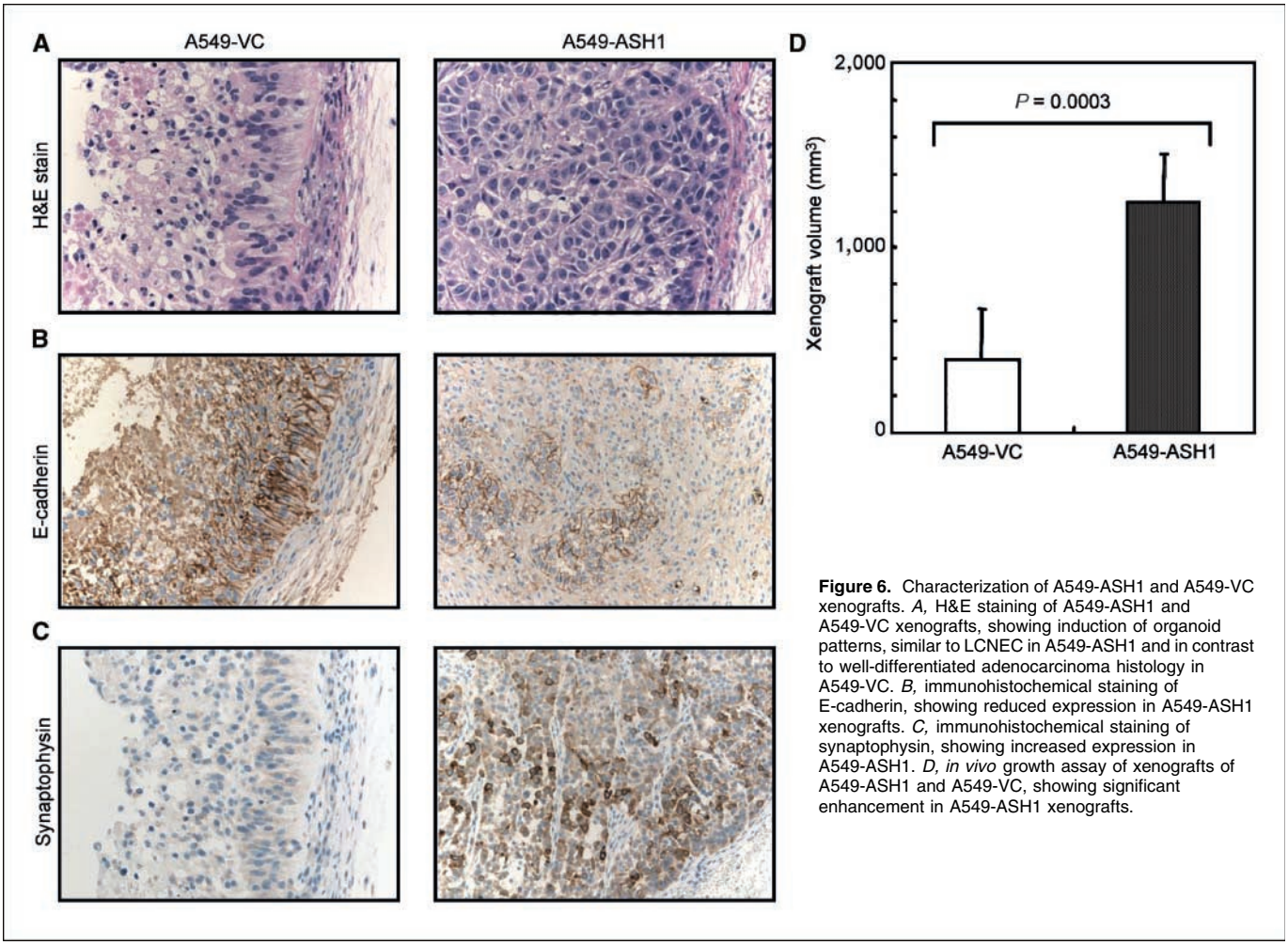

Figure 6. Characterization of A549-ASH1 and A549-VC xenografts. *A,* H&E staining of A549-ASH1 and A549-VC xenografts, showing induction of organoid patterns, similar to LCNEC in A549-ASH1 and in contrast to well-differentiated adenocarcinoma histology in A549-VC. *B,* immunohistochemical staining of E-cadherin, showing reduced expression in A549-ASH1 xenografts. *C,* immunohistochemical staining of synaptophysin, showing increased expression in A549-ASH1. *D, in vivo* growth assay of xenografts of A549-ASH1 and A549-VC, showing significant enhancement in A549-ASH1 xenografts.

that ASH1 expression may favor cancer cell growth through repression of DKK1 and DKK3 and the consequential activation of Wnt/β-catenin signaling. The present findings of frequent silencing of DKK1 in SCLCs, but not in NSCLCs, seem to be consistent with a recent report on the expression of DKK1 in NSCLCs (23).

E-cadherin promotes cell-cell interactions and sequesters β-catenin in the cell membrane, whereas reduced E-cadherin expression has been postulated to play a role in cell migration and metastasis, as well as anchorage independence (24). E-cadherin is silenced in a number of types of malignancy, including lung cancers with neuroendocrine features (25, 26). Several transcriptional repressors (the zinc finger proteins SNAI1/2 and ZEB1/2 and bHLH protein TWIST1) have been implicated in E-cadherin repression in cancers, which may in turn play a role in epithelial-mesenchymal transition (EMT) during tumor progression (27). Thus, our findings support the addition of ASH1 as a transcriptional repressor of E-cadherin. It is of interest that SCLC cells often show amoeboid migration through loose cell-cell and cell-matrix interactions, which may contribute to the acquisition of highly metastatic features by SCLCs (28). It is also notable that the morphologic features of A549-ASH1 cells resembled the amoeboid migration phenotype, possibly because of the ASH1-mediated reduction of E-cadherin and integrin β1 expression. Although down-regulation of E-cadherin is frequently associated with EMT, ASH1-induced phenotypic changes do not seem to conform to the strict criteria of EMT, because the induction of mesenchymal markers such as N-cadherin and vimentin was not observed in A549-ASH1 cells (data not shown). Alternatively, ASH1-induced phenotypic changes might reflect the cell migration capacity of neuronal progenitors during embryogenesis.

In summary, the present findings support the notion that ASH1 has a role in the development of lung cancers with neuroendocrine features, not only due to its decisive role as a transcriptional activator in neuroendocrine differentiation, but also because of its transcriptional repressor activity that has effects on various putative tumor suppressor genes. The latter repressor activity leads to the inactivation of genes related to negative regulation of cell growth, such as *DKK1*, which consequently activates Wnt/β-catenin signaling, as well as those related to cell adhesion, such as *E-cadherin* and *integrin β1*, which may also confer cell migration/metastasis capabilities. A future study of the molecular functions of ASH1 is warranted, which would shed light on its involvement in carcinogenic processes, as well as the underlying mechanism of the lineage-specific dependency of this dual function transcription factor in lung cancers with neuroendocrine features.

Acknowledgments

Received 8/27/2007; revised 11/6/2007; accepted 12/27/2007.

Grant support: Grant-in-aid for Scientific Research on Priority Areas from the Ministry of Education, Culture, Sports, Science and Technology of Japan and grant-in-aid for Scientific Research (C) from the Japan Society for the Promotion of Science.

The costs of publication of this article were defrayed in part by the payment of page charges. This article must therefore be hereby marked *advertisement* in accordance with 18 U.S.C. Section 1734 solely to indicate this fact.

We thank Dr. H. Miyoshi (RIKEN BioResource Center) for generously providing CSII-CMV-MCS-IRES2-Blasticidin and CSII-EF-MCS-IRES2-Venus vectors and Dr. A. Miyawaki (RIKEN Brain Science Institute) for generously providing the Venus (improved YFP) gene.

References

1. Osada H and Takahashi T. Genetic alterations of multiple tumor suppressors and oncogenes in the carcinogenesis and progression of lung cancer. Oncogene 2002;21:7421–34.
2. Travis WD, Rush W, Flieder DB, et al. Survival analysis of 200 pulmonary neuroendocrine tumors with clarification of criteria for atypical carcinoid and its separation from typical carcinoid. Am J Surg Pathol 1998;22:934–44.
3. Jones MH, Virtanen C, Honjoh D, et al. Two prognostically significant subtypes of high-grade lung neuroendocrine tumours independent of small-cell and large-cell neuroendocrine carcinomas identified by gene expression profiles. Lancet 2004;363:775–81.
4. Asamura H, Kameya T, Matsuno Y, et al. Neuroendocrine neoplasms of the lung: a prognostic spectrum. J Clin Oncol 2006;24:70–6.
5. Ball DW. Achaete-scute homolog-1 and Notch in lung neuroendocrine development and cancer. Cancer Lett 2004;204:159–69.
6. Linnoila RI. Functional facets of the pulmonary neuroendocrine system. Lab Invest 2006;86:425–44.
7. Borges M, Linnoila RI, van de Velde HJ, et al. An achaete-scute homologue essential for neuroendocrine differentiation in the lung. Nature 1997;386:852–5.
8. Linnoila RI, Zhao B, DeMayo JL, et al. Constitutive achaete-scute homologue-1 promotes airway dysplasia and lung neuroendocrine tumors in transgenic mice. Cancer Res 2000;60:4005–9.
9. Osada H, Tatematsu Y, Yatabe Y, Horio Y, Takahashi T. ASH1 gene is a specific therapeutic target for lung cancers with neuroendocrine features. Cancer Res 2005; 65:10680–5.
10. Garraway LA and Sellers WR. Lineage dependency and lineage-survival oncogenes in human cancer. Nat Rev Cancer 2006;6:593–602.
11. Osada H, Tatematsu Y, Masuda A, et al. Heterogeneous transforming growth factor (TGF)-β unresponsiveness and loss of TGF-β receptor type II expression caused by histone deacetylation in lung cancer cell lines. Cancer Res 2001;61:8331–9.
12. Shi Y and Whetstine JR. Dynamic regulation of histone lysine methylation by demethylases. Mol Cell 2007;25:1–14.
13. Ohm JE, McGarvey KM, Yu X, et al. A stem cell-like chromatin pattern may predispose tumor suppressor genes to DNA hypermethylation and heritable silencing. Nat Genet 2007;39:237–42.
14. Widschwendter M, Fiegl H, Egle D, et al. Epigenetic stem cell signature in cancer. Nat Genet 2007;39: 157–8.
15. Schlesinger Y, Straussman R, Keshet I, et al. Polycomb-mediated methylation on Lys27 of histone H3 pre-marks genes for *de novo* methylation in cancer. Nat Genet 2007;39:232–6.
16. Lee TI, Jenner RG, Boyer LA, et al. Control of developmental regulators by Polycomb in human embryonic stem cells. Cell 2006;125:301–13.
17. Boyer LA, Plath K, Zeitlinger J, et al. Polycomb complexes repress developmental regulators in murine embryonic stem cells. Nature 2006;441:349–53.
18. Clevers H. Wnt/β-catenin signaling in development and disease. Cell 2006;127:469–80.
19. Niehrs C. Function and biological roles of the Dickkopf family of Wnt modulators. Oncogene 2006;25: 7469–81.
20. Chamorro MN, Schwartz DR, Vonica A, et al. FGF-20 and DKK1 are transcriptional targets of β-catenin and FGF-20 is implicated in cancer and development. EMBO J 2005;24:73–84.
21. Gonzalez-Sancho JM, Aguilera O, Garcia JM, et al. The Wnt antagonist DICKKOPF-1 gene is a downstream target of β-catenin/TCF and is downregulated in human colon cancer. Oncogene 2005;24:1098–103.
22. Aguilera O, Fraga MF, Ballestar E, et al. Epigenetic inactivation of the Wnt antagonist DICKKOPF-1 (DKK-1) gene in human colorectal cancer. Oncogene 2006;25: 4116–21.
23. Yamabuki T, Takano A, Hayama S, et al. Dikkopf-1 as a novel serologic and prognostic biomarker for lung and esophageal carcinomas. Cancer Res 2007;67: 2517–25.
24. Derksen PW, Liu X, Saridin F, et al. Somatic inactivation of E-cadherin and p53 in mice leads to metastatic lobular mammary carcinoma through induction of anoikis resistance and angiogenesis. Cancer Cell 2006;10:437–49.
25. Salon C, Moro D, Lantuejoul S, et al. E-cadherin-β-catenin adhesion complex in neuroendocrine tumors of the lung: a suggested role upon local invasion and metastasis. Hum Pathol 2004;35:1148–55.
26. Pelosi G, Scarpa A, Puppa G, et al. Alteration of the E-cadherin/β-catenin cell adhesion system is common in pulmonary neuroendocrine tumors and is an independent predictor of lymph node metastasis in atypical carcinoids. Cancer 2005;103:1154–64.
27. Peinado H, Olmeda D, Cano A. Snail, Zeb and bHLH factors in tumour progression: an alliance against the epithelial phenotype? Nat Rev Cancer 2007;7:415–28.
28. Friedl P and Wolf K. Tumour-cell invasion and migration: diversity and escape mechanisms. Nat Rev Cancer 2003;3:362–74.
29. Takeuchi T, Tomida S, Yatabe Y, et al. Expression profile-defined classification of lung adenocarcinoma shows close relationship with underlying major genetic changes and clinicopathologic behaviors. J Clin Oncol 2006;24:1679–88.
30. Maeno K, Masuda A, Yanagisawa K, et al. Altered regulation of c-jun and its involvement in anchorage-independent growth of human lung cancers. Oncogene 2006;25:271–7. (Reference cited in Supplementary Materials and Methods).

Roles of Achaete-Scute Homologue 1 in DKK1 and E-cadherin Repression and Neuroendocrine Differentiation in Lung Cancer

Hirotaka Osada, Shuta Tomida, Yasushi Yatabe, et al.

Cancer Res 2008;68:1647-1655.